

LANDYNE

User Manual

Simulation on Polycrystalline SAED pattern
& Phase Identification

Copyright 2011-2024 LANDYNE ©

All Right Reserved

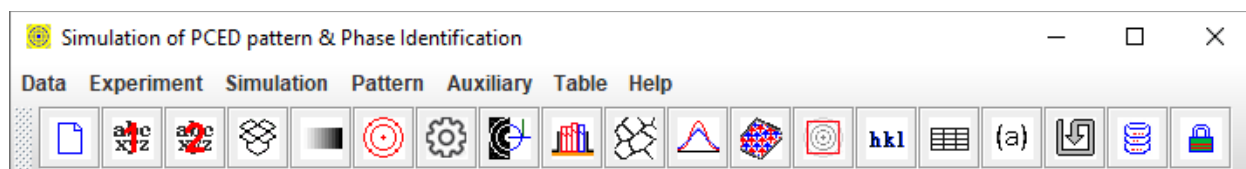


Table of Contents

1. Introduction.....	3
2. Theory background.....	4
2.1 Blackman's theory on the intensity of polycrystalline electron diffraction	4
2.2 Pseudo-Voigt function for peak profile.....	5
2.3 March Model for polycrystalline texture	5
3. The graphic user interface of PCED	8
3.1 Main interface.....	8
3.2 Menu and toolbar.....	9
4. Usage of PCED.....	9
4.1 Prepare new crystal structure file.....	10
4.2 Simulation	10
4.3 Index and intensity label	11
4.4 Phase Identification	12
4.5 Output for publication.....	13
5. Special topics on PCED	15
5.1 Partial occupancy factor and isotropic temperature factor	15
5.2 Load and center EDP.....	15
5.3 Peak profile, incident beam, and texture	15
5.4 Parameter table	16
5.5 Determine the weight ratio of a two-phase system	16
5.6 Grain size and the FWHM of diffraction ring.....	16
6. Examples.....	17
6.1 Phase identification of the Cr-N thin films	17
6.2 Analysis of thin films with FePt L1 ₀ phase.....	19
FePt film with a thickness of 20 nm	20
FePt film with thickness 4 nm	20

7. Installation of PCED	21
7.1 Installation	21
7.2 PCED in Landyne suite.....	21
7.3 License	21
8. References.....	21

1. Introduction

For polycrystalline or powder Transmission Electron Microscopy (TEM) specimens, electron diffraction ring patterns are widely employed for phase identification, where each diffraction pattern serves as a unique fingerprint for a known phase.

In the analysis of polycrystalline electron diffraction patterns, computer programs originally designed for powder X-ray diffraction can be adapted. One approach involves transforming electron diffraction ring patterns into integral intensity profiles as a function of scattering angle, enabling direct comparison with powder X-ray diffractograms. Alternatively, specialized computer programs utilize formulas for electron diffraction intensity to analyze raw or processed polycrystalline patterns. Integrated electron diffraction software often includes modules for simulating polycrystalline patterns, although direct comparison with experimental data for phase identification is rare. A dedicated computer program is crucial for efficiently and accurately performing this task.

The first version of PolyCrystalline Electron Diffraction (JEC/PCED, Li 2004) was developed to address these needs. Subsequent versions, such as ProJECT/PCED2 (Li, 2010), introduced new features including Blackman’s theory for intensity calculation, models for out-of-plane and in-plane texture matching, pseudo-Voigt functions for diffraction ring profiles, and improvements in pattern indexing and matching with experimental data. PCED2 integrated with the Landyne launcher and ProJECT package, offering enhanced user interface and input/output capabilities compared to its predecessor.

PCED3 introduced drag-and-drop functionality and enhanced image operations such as inversion, alignment, resizing, and rotation. PCED4 expanded capabilities to simulate two crystalline phases and implemented an indexing system for phase identification.

The current version, PCED6, further enhances manipulation of experimental electron diffraction patterns and improves indexing labels on simulated patterns. It includes tools for labeling and preparing figures for publication, significantly enhancing ease of use, especially for phase identification tasks. The software is implemented in openJDK and optimized for performance, including code obfuscation for security. A license file is required to fully unlock PCED6.jar for loading new input data files; otherwise, the program operates in demo mode using default input files (Al and Mg). Licenses can be obtained from LANDYNE computer software (jlandyne@gmail.com).

2. Theory background

The kinematic theory of electron diffraction is extensively covered in literature on texture analysis (e.g., Peng *et al.*, 2004). In this theory, the electron atom scattering factor is derived from the X-ray atom scattering factor using the Mott-Bethe relationship. Alternatively, it can be directly obtained from a parameterized table of electron atom scatter factors (Peng *et al.*, 1996), which is the method employed here.

Following the electron diffraction geometry, the radius of the diffraction ring, R , can be related to the length of the reciprocal vector $\mathbf{g}(hkl)$ as

$$R = \frac{L\lambda \sqrt{1 - \left(\frac{\lambda}{2d}\right)^2}}{1 - 2\left(\frac{\lambda}{2d}\right)^2} \quad (1)$$

Where L is the camera length, $d=1/|\mathbf{g}(hkl)|$ and λ is the wavelength of the incident electron beam.

The integrated intensity of reflections in the electron diffraction from the polycrystalline sample was derived in the book by Vainshtein (1964).

$$I = I_0 V \lambda^2 p \frac{F_{hkl}^2 d_{hkl}}{v_a^2 2} \quad (2)$$

Here V is sample volume, λ is the wavelength, p is a multi-factor, F_{hkl} is diffraction amplitude, the v_a is the volume of unit-cell, d_{hkl} is the (hkl) spacing.

2.1 Blackman's theory on the intensity of polycrystalline electron diffraction

Blackman's theory (Blackman, 1939) for polycrystalline electron diffraction intensity is rooted in the Bloch wave dynamic theory initially formulated by Bethe. It provides formulas for the integral intensity of two-beam dynamic diffraction. According to Peng *et al.* (2004), Blackman's theory represents an advanced approach in the field, despite its publication several decades ago. For detailed derivations of the formulas, readers are encouraged to consult the original paper. Below are some essential formulas:

The dynamical structure factor is given,

$$U_g = \frac{2meV_g}{h^2} \quad (3)$$

Where m is electron mass, e is the electron charge, h is Planck constant, V_g is Fourier coefficient of crystal potential.

The wave vector in a vacuum is given,

$$K_0^2 = \frac{2meE}{h^2} \quad (4)$$

Here E is the accelerated voltage of the electron microscope.

The wave vector inside the crystal is corrected with the mean inner potential,

$$K^2 = K_0^2 + U_0 \quad (5)$$

The diffraction intensity formulas can be given below in an integrated form considering there are angle distribution between the incident beam and the zone axis of the polycrystalline grains,

$$I_g^{integral} = I_o \frac{U_g}{gK^2} \int_0^A J_0(2x) dx \quad (6)$$

Where I_o is the intensity of the incident beam, U_g is dynamical structure factor, K is a wave vector and $J_0(x)$ the zero-order Bessel function and,

$$A = \frac{\pi U_g t}{K_n} \quad (7)$$

Here K_n is K normal component and $K^2 = K_n^2 + K_t^2$ (K_t is K component in the zero-order Laue zone).

The final intensity is an averaged integral intensity over K_n , considering the angle between the incident beam and the surface normal in a range from $-\frac{\pi}{4}$ to $\frac{\pi}{4}$.

2.2 Pseudo-Voigt function for peak profile

While the Voigt (V) function, a convolution of Gaussian (G) and Lorentzian (L) functions, is considered the most accurate for describing diffraction ring profiles, it is quite complex. As an alternative, the pseudo-Voigt (pV) function is commonly used, which is a linear combination of Gaussian and Lorentzian functions. According to Li (2007),

$$G(x) = h \exp(-4 \ln 2 \left(\frac{x - x_0}{FWHM}\right)^2) \quad (8)$$

$$L(x) = \frac{h}{1 + 4 \left(\frac{x - x_0}{FWHM}\right)^2} \quad (9)$$

$$pV(x) = \eta G(x) + (1 - \eta)L(x) \quad (10)$$

Here h is peak height, x_0 is peak position, FWHM is full width at half maximum. Figure 1 shows the comparison of profiles of Gaussian and Lorentzian functions.

2.3 March Model for polycrystalline texture

In powder samples, axially symmetric platy or capillary specimens composed of effective disk- or rod-shaped crystallites can exhibit textures influenced by their shape. Thin film samples often develop polycrystalline microstructures with preferred orientations either out-of-plane or in-plane during growth. Diffracted intensities from these orientations can be corrected or measured using a single pole-density profile.

For correcting powder X-ray diffraction affected by texture, the March model is commonly applied. This model, known for its simplicity and effectiveness, addresses both out-of-plane (platy) and in-plane (rod) textures.

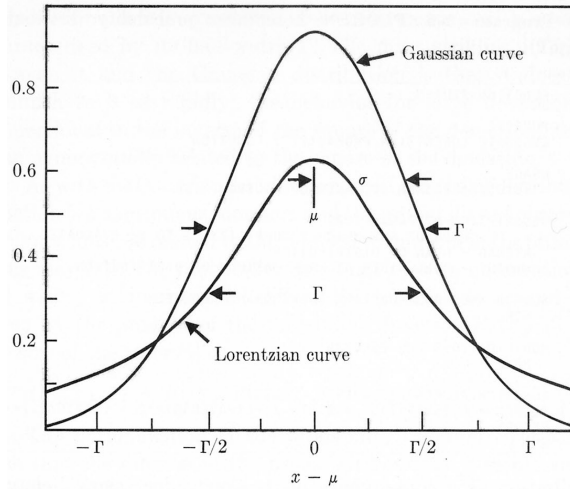


Figure 1. Comparison of profiles of Gaussian and Lorentzian functions.

The formulas were initially developed for X-ray powder diffraction and have been adapted for polycrystalline electron diffraction, considering the specific diffraction geometry of electron diffraction. Figure 2 illustrates example curves of the March functions used in X-ray powder diffraction (Bragg-Brentano geometry) and in polycrystalline electron diffraction for platy (out-of-plane) texture. The preferred zone axis density for polycrystalline electron diffraction, as described in Dollase (1986) (refer to Figure 1 in that paper), can be formulated as follows:

For out-of-plane texture,

$$P_g(O) = P_G(\alpha) = (r^2 \sin^2 \alpha + r^{-1} \cos^2 \alpha)^{-\frac{3}{2}} \quad (11)$$

For in-plane texture,

$$P_g(O) = \tilde{P}_G(\alpha) = \frac{2}{\pi} \int_0^{\frac{\pi}{2}} P_G(\alpha, \beta) d\beta \quad (12)$$

If the axial pole-density profile, $P(\varphi)$ is known, $\tilde{P}_G(\alpha)$ maybe obtained by numerical integration making use of the relation among coordinates: $\varphi = \cos^{-1}(\sin \alpha \cos \beta)$.

The intensity of polycrystalline electron diffraction including texture can be expressed as,

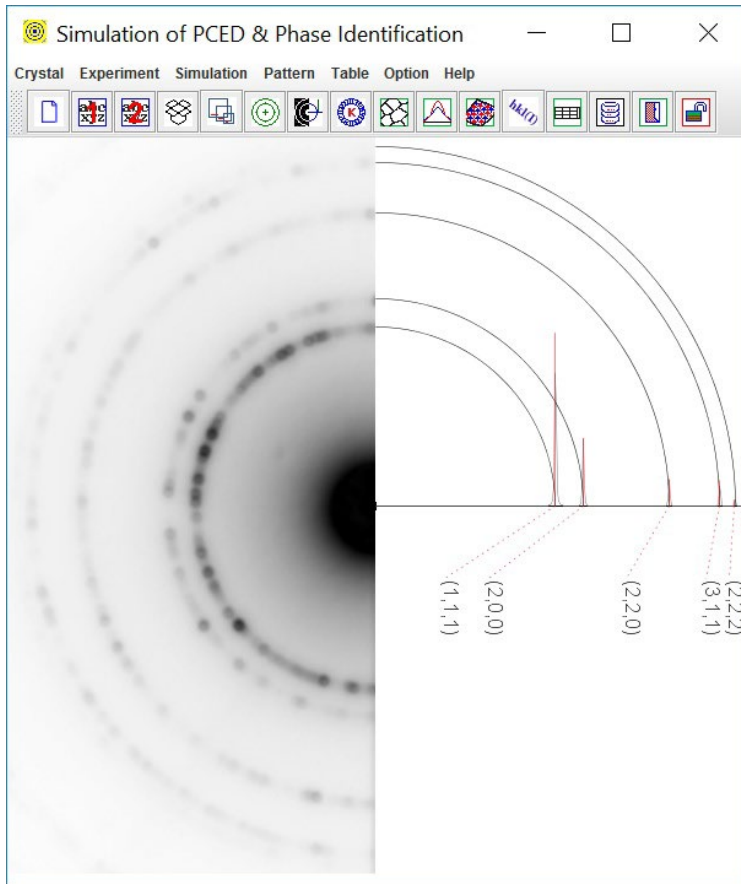


Figure 4. Snapshot of the primary interfaces of PCED, a phase identification using calculated polycrystalline electron diffraction pattern. The experimental PCED pattern is Al.

Where s is the scale factor, $P_g(\alpha_i)$ represents the density of $g(hkl)$ poles at the scattering vectors, and α_i denotes the angle between $G(HKL)$ and the i -th member of the symmetry-equivalent set of m diffraction planes. The preferred orientation plane itself belongs to a set of symmetry-equivalent planes. If the dominant morphological feature of the crystallites is re-indexed as another member of this set, the individual values of α_i in the above equation will be permuted, but the sum of terms remains unchanged. This sum can be interpreted as a generalized multiplicity term.

3. The graphic user interface of PCED

3.1 Main interface

The main interface of PCED6 is depicted in Figures 3 and 4, featuring both a menu and a toolbar for input parameter selection, and a frame to display simulation outputs. To simulate diffraction patterns using PCED6, users need to load structure data and configure input parameters, then simply click the "Run" button in the Calculation dialog (as shown later). For phase identification tasks, PCED6 requires loading experimental diffraction patterns first, followed by matching them with calculated patterns. The software supports loading two sets of structure data

simultaneously for comparison or simulation of two-phase systems. Users can adjust the software's frame size, including the display panel, through the Auxiliary menu.

3.2 Menu and toolbar

Menu and toolbar can be used to pop up dialogs for data and parameters. The toolbar can also be hidden. Most functions of the menu and toolbar are the same; some functions are only provided either in the menu or in the toolbar, e.g., the drag-and-drop box for loading EDP in formats of JPEG, PNG and TIFF.

Crystal menu provides an interface for preparing the new crystal data for loading the crystal data for phase 1 and phase 2. The file name can be viewed on the Parameter table in a dialog.

Experiment menu provides an interface to load experimental polycrystalline electron diffraction (PCED) pattern in JPEG, PNG and TIFF format. The loaded PCED pattern can be inverted the grey color and can also be erased. The pattern can be resized and rotated for the best display. The pattern can be shifted to view the scale bar and make the calibration of the simulation using a G-spacing marker. The pattern can be shown in full or half mode. The file name can be displayed or hidden.

Simulation menu provides a submenu for the choice of electron diffraction theories and several dialogs (e.g., average grain size, peak profile, texture model) for input parameters in the simulation. Two theories are used for the calculation of electron diffraction intensity. The kinematical theory is selected by default, and the second choice is Blackman's theory, which is an integral two-beam dynamic theory. Intensities calculated by Blackman's theory are more accurate than those calculated by kinematical theory, but the calculation of dynamic theory will take a longer time. A dialog of an index label is used to adjust the position and font size of the index. The conversion tool is for Miller and Miller-Bravais index for a hexagonal system. A dialog of parameter-table is used for monitoring the parameters in the calculation.

The pattern menu provided the output of the simulated patterns, the hkl intensity list, the preference of the hkl-inten list file, and print to a printer or a PDF file when a PDF print driver was installed.

Options menu provides the look-and-feel provided by Java; an option to hide or show toolbar; freedom of customizing the appearance of simulated pattern; for example, the diffraction peak and ring color, the curve or solid profile; set the reciprocal spacing for a marker.

The help menu provides a tool to find the current driver and its serial number (S.N.), a table of space group numbers and symbols, version information.

4. Usage of PCED

The recommended way is to use Landyne launcher. In the following, we show step by step from preparing structure data file, common routine usage for simulation, and to the last steps of saving and printing the results. More details on specific topics are left in the next section.

4.1 Prepare new crystal structure file

A structure data file can be prepared using the **New Crystal Structure File** dialogue window in Figure 5. The dialogue window provides an automatic assistant for the user and makes sure to meet the requirement of the file format. The template is embedded with the 230 space groups in the Hermann-Mauguin notation, which list in the international table for crystallography. However, only b unique axis will be used in a monoclinic system. Two origin choices can be accepted as input parameters, but choice-2 will be converted to choice-1. To save the data structure, click the **Save** button; or make a new one click the **New** button.

atom	elem #	x	y	z	occ.
		0.0	0.0	0.0	1.0

Figure 5. Snapshot of the preparation of the new crystal structure file.

The crystal file can be also converted from previous data for modification or from a crystallographic information file (CIF). If a data file in an alternative setting of space group for triclinic, monoclinic and orthorhombic systems is used, please click on the alternative settings (1~74). A tool for the transformation of files from the nonconventional notations to the standard notations is provided.

4.2 Simulation

The kinematical theory is used as a default selection in the simulation since it is fast and fewer input parameters are required. Integral dynamical two-beam theory (Blackman's theory) can be turned on using the **Theory** submenu in the **Simulation** menu.

Basic parameters for calculation and adjustment of the diffraction pattern can be filled in or changed in the **Calculation** dialog in Figure 6. To generate new diffraction pattern needs, click the **Run** button. The pattern is automatically updated, corresponding to the change of other parameters.

Mass ratio defines relative masses of the two phases when the fields of phase1 and phase2 are checked.

Volume ratio defines relative volumes of the two phases when the fields of phase1 and phase2 are checked.

g-spacing zoom and **Intensity scale** simulated the camera length and the exposure time in the experiment, which is used to make a better appearance of the calculated pattern.

Peak type can be chosen from the integral intensity on a ring or intensity on unit-arc-length.

The diffraction diagram can be viewed as **peak** and **profile** separately or together.

Diffraction rings can be viewed as either a ring to match the experiment pattern or only the top half in order to clearly show the index without intervening or without a ring at all.

The diffraction ring's appearance is also controlled by the profile intensity (**intensity threshold**).

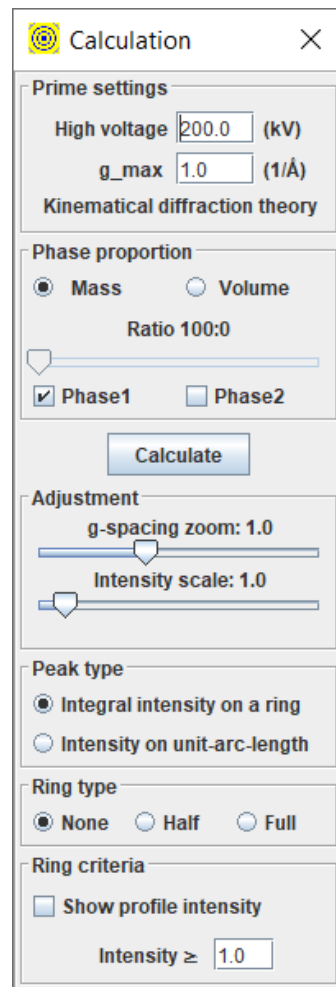


Figure 6. Snapshot of the calculation dialog.

4.3 Index and intensity label

There are cases where diffraction peaks are quite dense; the index labels may be overlapped when they are shown by the side of the diffraction diagram, especially for the diffraction diagram of the two-phase system. It is essential to allow users to adjust the positions of the index (and intensity) labels.

To avoid the situation, PCED is allowed to select the location of an index label and to spread it when necessary. In the **Index Label dialog**, a top point can be viewed when the checkbox of the **Top point** is selected and moved around with mouse drag-and-drop. Dash line can be viewed

when the **Baseline's** checkbox is selected and moved up/down by the mouse wheel or the arrow keys (after clicking the panel).

Figure 7 illustrates the process of adjusting the positions of index labels using the Label dialog, which includes the following functionalities:

- **Remove weak peaks:** Allows removal of indexes for weak diffraction peaks by adjusting the intensity threshold (arbitrary unit).
- **Position adjustment:** To adjust index label positions:
 - Select either phase 1 or phase 2.
 - Check the "Index" box for the phase selected.
 - Check the "Guidelines" box for reference lines (optional).
 - Choose between "Top point" or "Baseline" for alignment.
 - Use drag-and-drop operations with the mouse pointer to move index labels to desired positions.
- **Font size:** Set the font size independently for phase 1 and phase 2.
- **Link lines:** Toggle link lines on or off as needed.

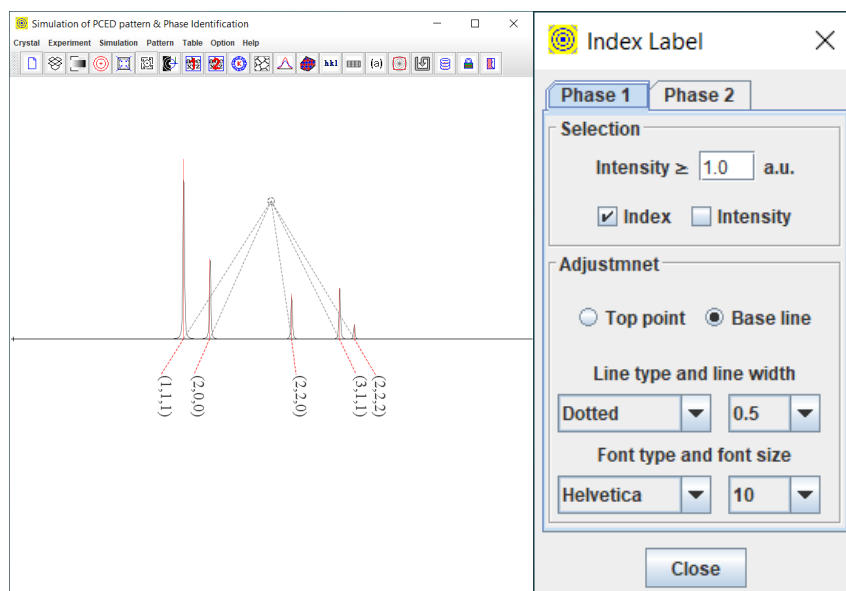


Figure 7. Example for the Label adjustment. Snapshot of the Label adjustment dialog.

4.4 Phase Identification

It is easy to make a phase identification using PCED. An experimental PCED pattern and the crystal data of the possible phases are needed. The PCED pattern is in JPEG (.jpg), PNG (.png) or TIFF (.tif) formats, which can be quickly loaded using the window file system in a menu or the drag-and-drop box in the graphic menu bar. The PCED pattern can be processed, such as resize, rotate, and center, as shown in Figure 8. The scale-bar on the PCED pattern can be used for calibration of the G-spacing zoom in Figure 9. The PCED pattern can be displayed in full or

half size. The simulation of the possible phases is then calculated on the right side of the pattern panel if the positions and intensities of the diffraction rings are matched in agreement with the experimental PCED pattern.

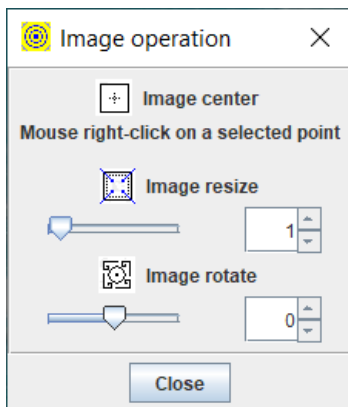


Figure 8. Snapshot of the image operation, such as alignment, resize, and rotation.

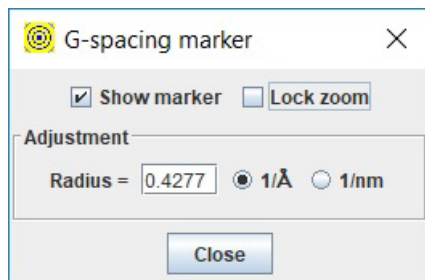


Figure 9. Snapshot of the G-spacing marker.

Phase identification is made; otherwise, the next possible phase is loaded for a check until all possible phases are run out.

For the hexagonal system, the index can be the three-index Miller notation or the four-index Miller-Bravais notation. Three-index Miller notation is used in the PCED. A tool for converting the Miller notation and Miller-Bravais notation is also provided, as shown in Figure 10.

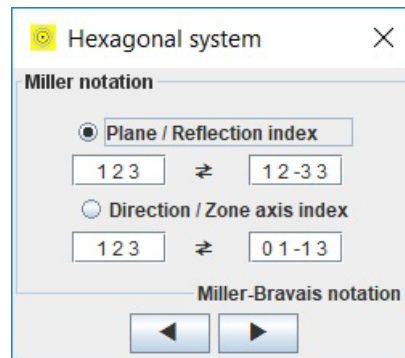


Figure 10. Snapshot of the Hexagonal system index.

4.5 Output for publication

Calculated diffraction data can be saved into a file using **Save** in **File** menu, in which it includes hkl and intensity (per unit-length) together with the parameters used in the simulation as a default option. More info, such as length of a reciprocal vector (g), crystalline plane spacing (d), intensity (per unit angle), can be chosen to be saved by using **selection in hkl-inten** dialog in the options menu.

Simulated diffraction patterns and preloaded experimental patterns can be saved as output files in JPEG, PNG, or TIFF format. The output size can be selected according to the region of interest (ROI) and the point per inch (PPI). A tool for figure label is available, so the figure in one-step to be used for publication. An example figure and the tool for the figure label are shown in Figure 11.

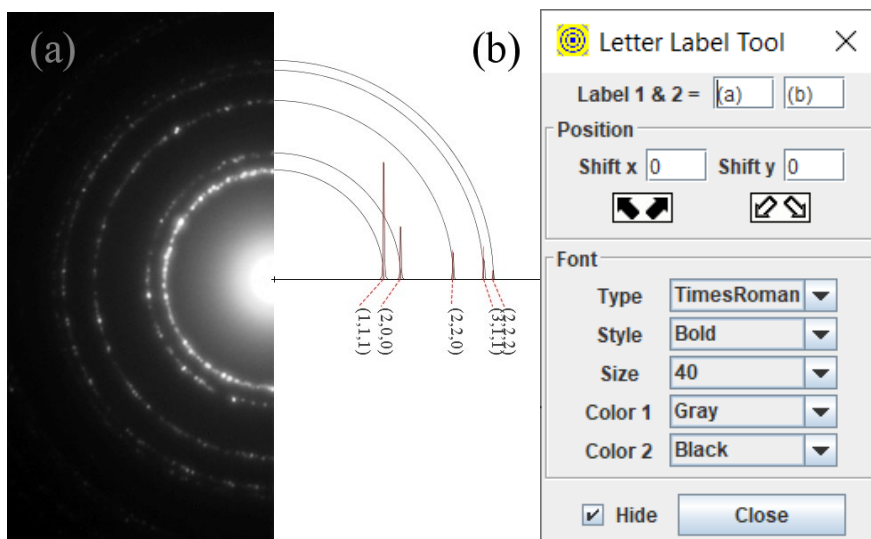


Figure 11. Snap-shot of output and a tool for figure label.

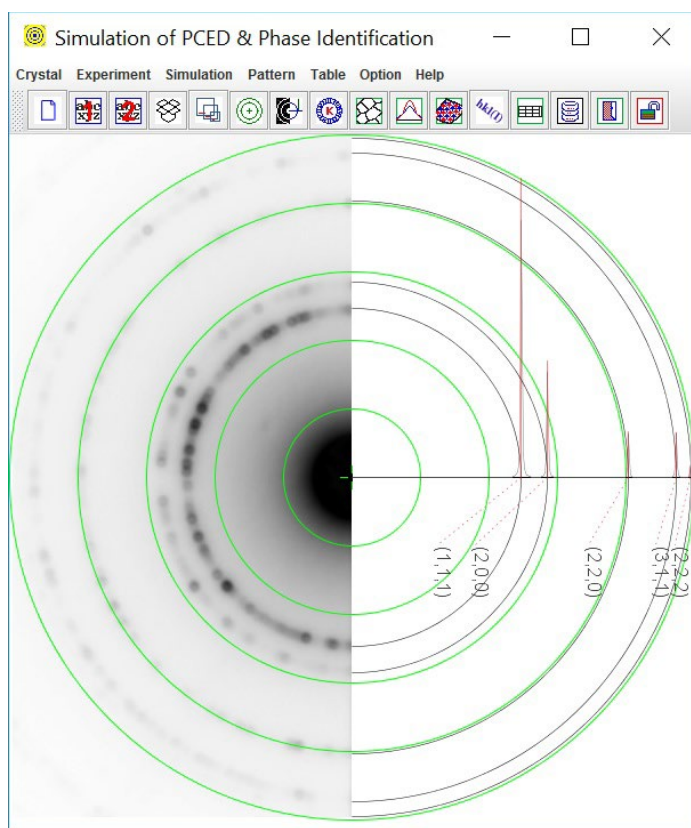


Figure 12. Snapshot of experimental pattern processing, resize, rotation, and center.

5. Special topics on PCED

5.1 Partial occupancy factor and isotropic temperature factor

In crystalline structures, some atom coordinates may not be fully occupied. In such cases, the occupancy factor (default value 1.0) should be adjusted according to the specific crystalline structure when preparing data files for polycrystalline electron diffraction simulations.

Partial occupancy factors can also be employed to simulate varying degrees of chemical order within a structure. For instance, in the case of the chemically ordered FePt L10 phase (see section 6), different types of atoms may share the same atomic coordinates with different occupancy factors based on their chemical ratio. Notably, the sum of the occupancy factors for these atoms always equals 1.0.

The isotropic temperature factor is utilized to model the effects of lattice vibrations, following the Debye model. While this model is a simplified approximation, it effectively simulates the decrease in diffraction intensity as the absolute value of the scattering vector $|g|$ increases. Higher values of $|g|$ correspond to greater reductions in diffraction intensity.

5.2 Load and center EDP

For phase identification, the experimental polycrystalline electron diffraction pattern must be loaded and compared with simulated patterns calculated from related phase files. The experimental pattern should be in JPEG, PNG, or TIFF formats. You can load the experimental pattern using the "Load" option in the Experiment menu or by using the drag-and-drop feature. After loading, you can resize, rotate, or center the pattern.

To center the pattern precisely, use the "Shift & Center" function. This action will display concentric circles on the main panel. Click and hold the left mouse button to drag the pattern to the desired center position within the panel (refer to Figure 12). Click "Shift & Center" again to lock the PCED pattern in place and hide the concentric circles. Fine adjustments may be necessary to achieve the exact positioning. You can adjust the number of concentric circles displayed using the "Number of Reference Circles" option.

5.3 Peak profile, incident beam, and texture

The profile of the diffraction ring's cross-section, known as the peak profile, can be simulated using a pseudo-Voigt function along with parameters like grain size (diameter) and a constant K. The ratio of Gaussian and Lorentzian functions in the pseudo-Voigt function can be adjusted using the "Peak Profile" option found in the Simulation menu (default value is 0.5).

To further refine the simulation, you can adjust the grain size (diameter) and the constant K using the "Average Grain Size" dialog in the Simulation menu.

In polycrystalline electron diffraction, the incident beam is often much stronger compared to the diffraction rings, potentially obscuring weaker rings near the incident beam. To address this, the

incident beam can be included in the simulated pattern by checking the "Included" box in the Peak Profile dialog. You can then adjust its shape by modifying the corresponding height and full width at half maximum (FWHM) values.

You have the option to select the peak and profile individually, and the style of the profile can be chosen between solid shadow or curve representations.

5.4 Parameter table

In the texture dialog of PCED6, you can input the axis of texture and the March parameter (default value 1.0 for full randomness). These values can be separately set for phase 1 and phase 2.

The March parameter r is used to quantify the degree of randomness in polycrystalline or powder samples. A higher value of r indicates better approximation to randomness. Conversely, to describe the level of preferred orientation, we suggest using the reversed March parameter $r'=1.0-r$. Thus, $r'=0$ represents full randomness, and higher values of r' indicate stronger preferred orientation, with $r'=1.0$ representing perfect alignment.

To facilitate tracking and management of simulation parameters, you can use the "Parameter Table" option in the Simulation menu. This table lists essential parameters for both phase 1 and phase 2, providing convenience in parameter management during simulations.

5.5 Determine the weight ratio of a two-phase system

PCED6 offers a method to simulate the composite diagram of a two-phase system with a specified weight ratio. The program utilizes a formula to convert the weight ratio into the numbers of unit cells in diffraction, using the atomic weight per unit cell for each phase for simplicity.

To experimentally determine the weight ratio of a two-phase system, calibration using a standard sample with a known weight ratio is essential. This calibration ensures accurate interpretation and simulation of diffraction patterns in PCED6.

5.6 Grain size and the FWHM of diffraction ring

PCED6 provides a method to simulate the Full Width at Half Maximum (FWHM) of diffraction rings based on a given average grain diameter and K factor. The FWHM values for each ring in the calculated diagram are consistent with the pseudo-Voigt function used in the simulation.

In experimental diffraction patterns, the diffraction rings often consist of individual spots from grains with varying grain sizes. The peak profiles are determined by summing data around each ring. Therefore, different pseudo-Voigt functions may be required to fit the peaks of each ring accurately.

The grain size does not directly influence the peak profiles of polycrystalline electron diffraction ring patterns in a straightforward manner. Grain size measurements are typically conducted using bright field or dark field imaging methods.

6. Examples

6.1 Phase identification of the Cr-N thin films

According to the phase diagram of the Cr-N system (Venkatraman & Neumann, 1990), the Cr₂N phase is stable within a nitrogen composition range of approximately 27.5–33 at. %, while the CrN phase has a very narrow equilibrium range of 47.5–50 at. % N. CrN crystallizes in a face-centered cubic (f.c.c.) structure with a lattice parameter of $a=0.414$ nm, whereas Cr₂N adopts a hexagonal structure with lattice parameters $a=0.4752$ nm and $c=0.4429$ nm (Villars & Calvert, 1985).

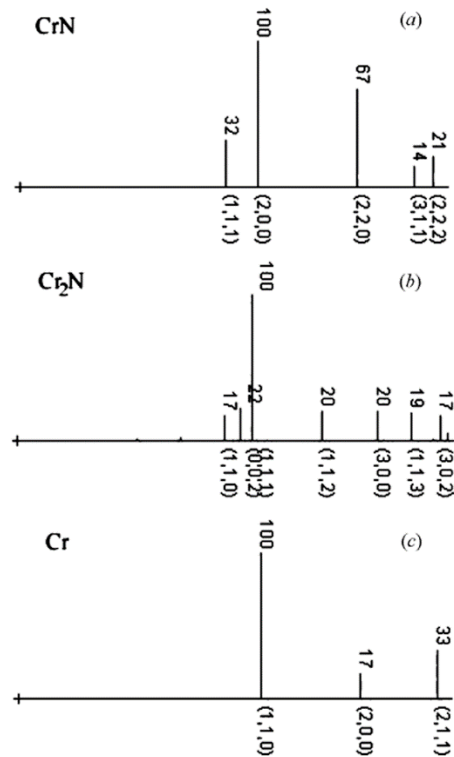


Figure 13. Comparison of calculated polycrystalline electron diffraction patterns of (a) f.c.c. CrN, (b) hexagonal Cr₂N and (c) b.c.c. Cr, with intensities (b) on top and indices at the bottom of each peak.

Cr-N thin films have been extensively investigated as important coating materials. Our research on Cr-N films originated from the study of Cr-doped AlN (AlCrN), a system known for its ferromagnetic semiconductor properties. To ascertain the origin of ferromagnetism, it was crucial to exclude contributions from any potential second phases in AlCrN, such as CrN and

Cr₂N. Therefore, detailed studies were conducted on the structure and properties of Cr–N films (Li *et al.*, 2004).

Cr–N films were deposited on Si (001) substrates by reactive magnetron sputtering under an N₂/Ar atmosphere at room temperature. The composition of the films, denoted as Cr_{1-x}N_x, was varied by adjusting the N₂/Ar pressure ratio during the synthesis process. Two batches of thin films were prepared with different N₂ partial pressures: sample 1, P(N₂) = 5 x 10⁻¹ Pa and sample 2, P(N₂) = 5 x 10⁻³ Pa.

Simulation of the polycrystalline electron diffraction patterns from CrN and Cr₂N and Cr

Figure 13 displays the simulated polycrystalline electron diffraction patterns for (a) face-centered cubic (f.c.c.) CrN phase (Villars & Calvert, 1985), (b) hexagonal Cr₂N phase (Kim *et al.*, 1990), and (c) body-centered cubic (b.c.c.) Cr phase. The calculated patterns illustrate the distinguishable features of CrN, Cr₂N, and Cr phases in polycrystalline electron diffraction.

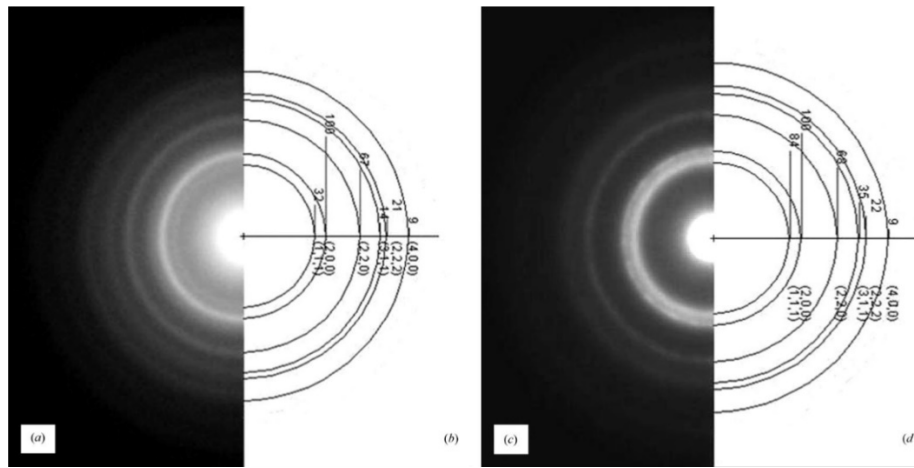


Figure 14. Experimental polycrystalline electron diffraction patterns of thin films produced (a) with N₂ partial pressure P(N₂) = 5 x 10⁻¹ Pa and (c) with N₂ partial pressure P(N₂) = 3 x 10⁻³ Pa. Simulated patterns (b) based on the cubic CrN structure and (d) based on the cubic CrN structure with half occupancy of N sites.

Thin films produced with different N₂ partial pressure

Figure 14 presents the following: (a) a polycrystalline electron diffraction pattern from sample 1 and (b) a simulated pattern based on the structure of the face-centered cubic (f.c.c.) CrN phase. The agreement in both ring radii and relative intensities confirms that the microcrystalline phase in sample 1 is indeed the f.c.c. CrN phase. Figure 14(c) displays a polycrystalline electron diffraction pattern from sample 2. The simulated patterns (see Figs. 13b and 13c) corresponding to the hexagonal Cr₂N phase and b.c.c. Cr do not match the experimental pattern. While the ring radii in the experimental pattern are similar to those in Fig. 14(a), the relative intensities differ. Hence, the microcrystalline phase in sample 2 likely shares the same or very similar unit cell and lattice parameters as sample 1.

Given that sample 2 was synthesized under a lower N₂ partial pressure compared to sample 1, we attempted to interpret Fig. 14(c) using the structure of cubic CrN phase with vacancies at N sites. A simulated pattern (Fig. 14(d)) calculated with the structure of cubic CrN phase featuring half-occupancy at N sites demonstrates a significant increase in intensity of the innermost ring, while other rings show minimal intensity changes. This simulated pattern in Fig. 14(d) effectively matches the experimental one in Fig. 14(c), suggesting that the microcrystalline phase in sample 2 can be identified as cubic CrN phase with vacancies at N sites.

6.2 Analysis of thin films with FePt L₁₀ phase

To enhance the areal density of magnetic recording media, reducing the grain size of magnetic films is crucial. Achieving a high-anisotropy material is essential for ensuring thermal stability in the new media. The FePt L₁₀ phase stands out due to its high anisotropy energy, making it a promising candidate for magnetic recording applications. Initially, as-deposited FePt films typically exist in a disordered face-centered cubic (fcc) phase, which is magnetically soft. However, through suitable annealing treatments, this phase can be transformed into the ordered L₁₀ phase.

The chemical ordering within the L₁₀ phase is influenced by the film's composition and the specific conditions during heat treatment. For optimal data-storage applications, it is advantageous for the [001] axis of the L₁₀ phase to be oriented perpendicular to the film plane. This orientation is favored because the [001] axis of the L₁₀ phase represents an easy magnetic axis, ensuring efficient magnetic recording.

One effective method to achieve the desired (001) texture involves depositing a multilayer of Fe and Pt films followed by annealing at elevated temperatures. Researchers have focused on understanding the formation of (001) texture across various ranges of film thicknesses to optimize magnetic properties for practical applications. This approach aims to control the growth and orientation of grains within the film, thereby enhancing magnetic performance and stability in magnetic recording media.

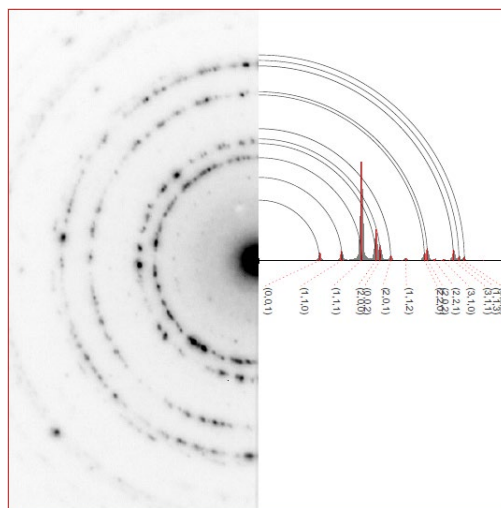


Figure 15. SAED pattern of the FePt L₁₀ phase in a film with a thickness of 20 nm annealed at 600 °C for 30 seconds and calculated pattern for phase identification.

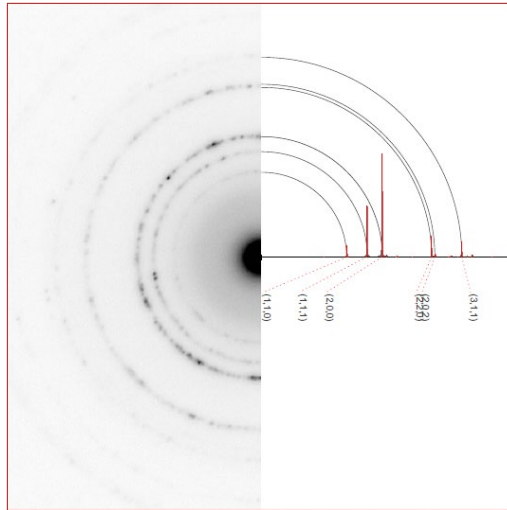


Figure 16. SAED pattern of the FePt L₁₀ phase in a film with a thickness of 4 nm annealed at 600 °C for 30 seconds and calculated pattern with (001) texture.

FePt film with a thickness of 20 nm

Figure 15 shows the SAED pattern of FePt film with a thickness of 20 nm annealed at 600 °C for 30 seconds and the calculated pattern of the FePt L₁₀ phase-in for phase identification. The ring radiuses and corresponding intensities in the calculated pattern are considered to match well with the experimental pattern. On the other hand, the ring radiuses and corresponding intensities in the calculated pattern with FePt fcc polycrystals (not shown here) do not match the experimental pattern. Thus, the phase is confirmed to be the chemical ordered FePt L₁₀ phase.

FePt film with thickness 4 nm

The radius step of the diffraction patterns in Figure 15 is the same as those in Figure 16; however, the intensity distributions of the diffraction patterns are dramatically different. Now we estimate the (001) texture of the film with a thickness of 4 nm semi-quantitatively.

Fig.17 is a processed digital diagram of Fig.16 using a program QPCED (Li, 2007). Using March parameters of 0.45 and a given chemical order (Pt sites with 80%Pt+20%Fe; Fe sites with 80%Fe+20%Pt), a calculated diagram in Fig.18 is best matching with Figure 17 is obtained. As discussed in section 5.3, if we use revised March (0.0 for full random and 1.0 for perfect texture), the texture can be described as 55% of the (001) texture.

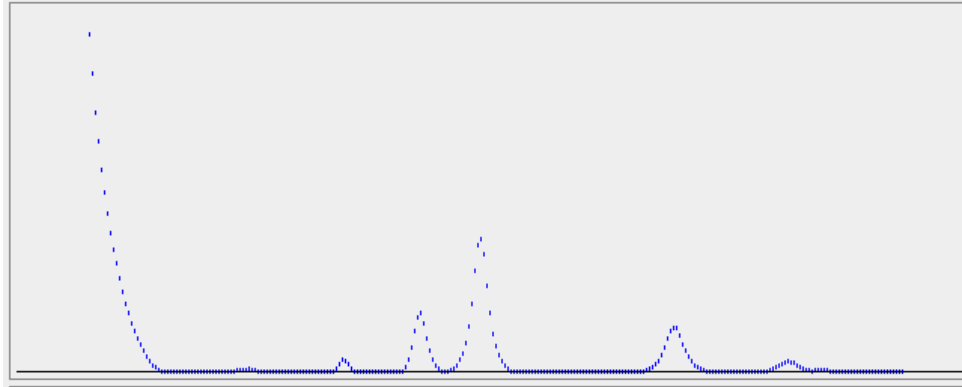


Figure 17. Digital processed diagram of the experimental electron diffraction pattern in Figure 17.

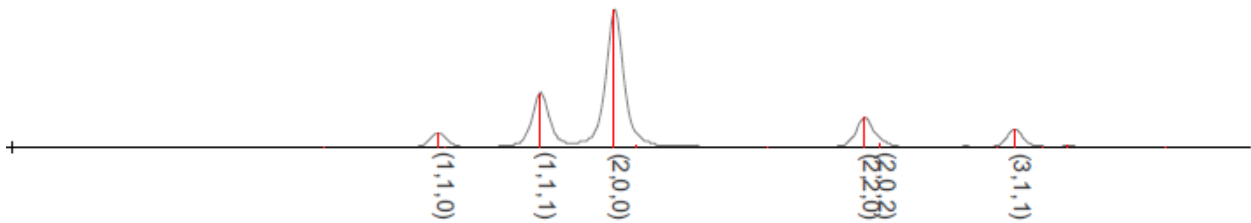


Figure 18. A simulated diffraction diagram fitting to Figure 17 reveals the degrees of chemical order and (001) texture of film with a thickness of 4nm.

7. Installation of PCED

7.1 Installation

Download and install the most recent openJDK from the internet. Download (<https://landyne.com>) and decompress the Landyne6 package. Copy the license to the programs\ subfolder.

7.2 PCED in Landyne suite

Click the PCED in Landyne launcher to start the software.

7.3 License

A license file is needed to unlock the program (PCED.jar) for simulating PCED patterns. The program may run in demo mode, which works in full functions but limits to the given crystal files. A license is available from LANDYNE (computer software and graphic design).

8. References

Blackman M., On the Intensities of Electron Diffraction Rings. Proceedings of the Royal Society of London, Series A, Mathematical and Physical Sciences, 173 (1939) 68-82.

Dollase W.A., Correction of Intensities for Preferred Orientation in Powder Diffractometry: Application of the March Model. *J. Appl. Cryst.* 19 (1986) 367-272.

Kim, S.-J., Marquart, T. & Franzen, H. F., *J. Less Common Met.* 158 (1990) L9–L10.

Li X.Z., Zhang J., Sellmyer D.J., TEM study of crystalline structures of Cr-N thin films. *Journal of Applied Crystallography*, 37 (2004) 1010-1012.

Li X.Z., JECPCED—a computer program for simulation of polycrystalline electron diffraction pattern and phase identification. *Ultramicroscopy* 99 (2004) 257-261.

Li X.Z., Quantitative Analysis of Polycrystalline Electron Diffraction Patterns, *Microanalysis and Microscopy* 2007.

Li X.Z., PCED2.0 - A computer program for advanced simulation of polycrystalline electron diffraction pattern. *Ultramicroscopy* 110 (2010) 297-304.

Peng L.M., Dudarev S. L., and Whelan M. J., *High Energy Electron Diffraction and Microscopy*, Oxford University Press (01/01/2004).

Peng L.M., Ren G., Dudarev S.L., and Whelan, M.J., Robust Parameterization of Elastic and Absorptive Electron Atomic Scattering Factors, *Acta Cryst. A*52 (1996) 257-276.

Vainshtein B.K., *Structure Analysis by Electron Diffraction*, translated and edited by Feigl E. and Spink J.A., Pergamon Press, Oxford (1964).

Venkatraman, M. & Neumann, J. P., *Binary Alloy Phase Diagrams*, 2nd ed., edited by T. B. Massalski, H. Okamoto, P. R. Subramanian & L. Kacprzak. Materials Park, Ohio: ASM. (1990).

Villars, P. & Calvert, L. D., *Pearson's Handbook of Crystallographic Data for Intermetallic Phases*. Materials Park, Ohio: ASM. (1985).